2

Basic Material Quartz and Related Innovations

A. Ballato

2.1 General

2.1.1 Commercial and Technological Usages of Quartz

Although material quartz is of scientific interest in its own right, its volume of usage and variety of applications dictate its technological importance. The technological prominence of α-quartz stems largely from the presence of piezoelectricity, combined with extremely low acoustic loss. It was one of the minerals with which the Brothers Curie first established the piezoelectric effect in 1880. In the early 1920s, the quartz resonator was first used for frequency stabilization. Temperature-compensated orientations (the AT and BT shear cuts) were introduced in the 1930s, and assured the technology's success. By the late 1950s, growth of cultured bars became commercially viable, and in the early 1970s, cultured quartz use for electronic applications first exceeded that of the natural variety. The discovery of cuts that addressed compensation of stress and temperature transient effects occurred in the 1970s, and led to the introduction of compound cuts such as the SC, which has both a zero temperature coefficient of frequency, and is simultaneously stress-compensated [1–5]. Between 10^9 and 10^{10} quartz units per year were produced by 2000 at frequencies from below 1 kHz to above 10 GHz. Categories of application include resonators, filters, delay lines, transducers, sensors, signal processors, and actuators. Particularly noteworthy are the bulk- and surface-wave resonators; their uses span the gamut from disposable timepieces to highest precision oscillators for position-location, and picosecond timing applications. Stringent high-shock and high-pressure sensor operations are also enabled. Table 2.1 shows the major applications of quartz crystals. These applications are discussed subsequently in greater detail. For general background and historical developments, see [1, 6–11].

Crystal quartz for timekeeping currently has a global market of over 10^9 USD per year, and that for cellular communications exceeds 50×10^9 USD

Table 2.1. Major applications of quartz crystals

Military and aerospace	Research and metrology	Industrial	Consumer	Automotive
– Communications – Navigation/GPS – IFF – Radar – Sensors – Guidance systems – Fuzes – Electronic warfare – Sonobuoys	– Atomic Clocks – Instruments – Astronomy and geodesy – Space tracking – Celestial navigation	– Communications – Tele-communications – Mobile/cellular/portable radio, telephone, and pager – Aviation – Marine – Navigation – Instrumentation – Computers – Digital systems – Displays – Disk drives – Modems – Tagging/identification – Utilities	– Watches and clocks – Cellular and cordless phones, pagers – Radio and hi-fi equipment – Color TV – Cable TV systems – Home computers – VCR and video camera – CB and amateur radio – Pacemakers – Toys and games	– Engine control, stereo, clock – Trip computer – Navigation/GPS

per year. Useful rules-of-thumb for the temporal evolution of this technology are the following:

- Upper frequency limit: $f_0 = 10^{+r}$, where f_0 is nominal frequency, $r = 4 + 0.075\ (Y - 1920)$, and Y is year.
- Frequency accuracy (total fractional absolute frequency variations over all environmental ranges such as temperature, mechanical shock, and aging): $\Delta f/f_0 = 10^{-a}$, where $\Delta f = (f - f_0)$ is frequency shift, and $a = 3.5 + 0.05\ (Y - 1940)$.
- Aging: $<10^{-8}$/day for production units, and $<10^{-11}$/day for high precision units.
- Frequency stability: $\Delta f/f_0 = 10^{-s}$, where $s = 6 + 0.1(Y - X)$, with $X = 1920$ for laboratory versions, $X = 1940$ for commercial versions, and $X = 1960$ for large-scale production models. Observation times are in the range 0.1–10 s. As with Moore's Law, a saturation of these exponential rates is predicted, but not yet observed.

2.1.2 Phases of the Silica System [12–15]

Silica (SiO_2) is the second most abundant molecule on earth, after H_2O. The phase diagram of the silica system is sketched in Fig. 2.1. This chapter discusses some of the properties and applications of the commercially significant α-quartz phase. Other phases appearing in the diagram are mentioned briefly below.

"Quartz" refers to crystalline α-SiO_2, arranged in point group symmetry 32 (Hermann-Mauguin)/D_3 (Schönflies). Figure 2.2 indicates its symmetry elements; z (x_3) is the axis of threefold symmetry. Three equivalent secondary axes x (x_1) are parallel to the twofold axes, and perpendicular to the x_3 axis; three equivalent y (x_2) axes are normal to x_3 and to the respective x_1 axes. The trigonal axis is denoted "optical" (x_3 a screw axis, rotating polarized light), the digonal (x_1) axes are denoted "electrical" and are piezoelectrically active; the x_2 axes are "mechanical" axes. Axial and sign conventions are given in various IEEE Standards and related papers [16–22].

The interlocking nature of the lattice bonds leads to a strong, rigid structure with scratch hardness of 0.667 (with alumina unity), and Moh hardness 7. Si–O bonds occur in pairs with lengths of 0.1598 and 0.1616 nm. Four oxygens coordinate each silicon, with each oxygen slightly off a line joining two neighboring silicons. Bonding is ∼0.6 covalent and 0.4 ionic, with average bond energies ∼4.85 eV/bond (∼0.468 MJ mol^{-1}), whereas a single Si–O bond has an energy of 3.82 eV [23]. The unit cell lattice constants are $a_o = 0.4913$ nm, and $c_o = 0.5404$ nm at room temperature [1, 14, 15, 24]. Quartz exhibits enantiomorphism, with chiral (left/right) pairs having space groups $P3_121/D_3{}^4$ and $P3_221/D_3{}^6$. Figure 2.3 portrays the external facet arrangement of a completely developed, right-handed specimen.

Upon heating, α-SiO_2 ("low quartz") undergoes a phase transition at 573.3°C, becoming β-SiO_2 ("high quartz"); in the transition, the silicon atoms

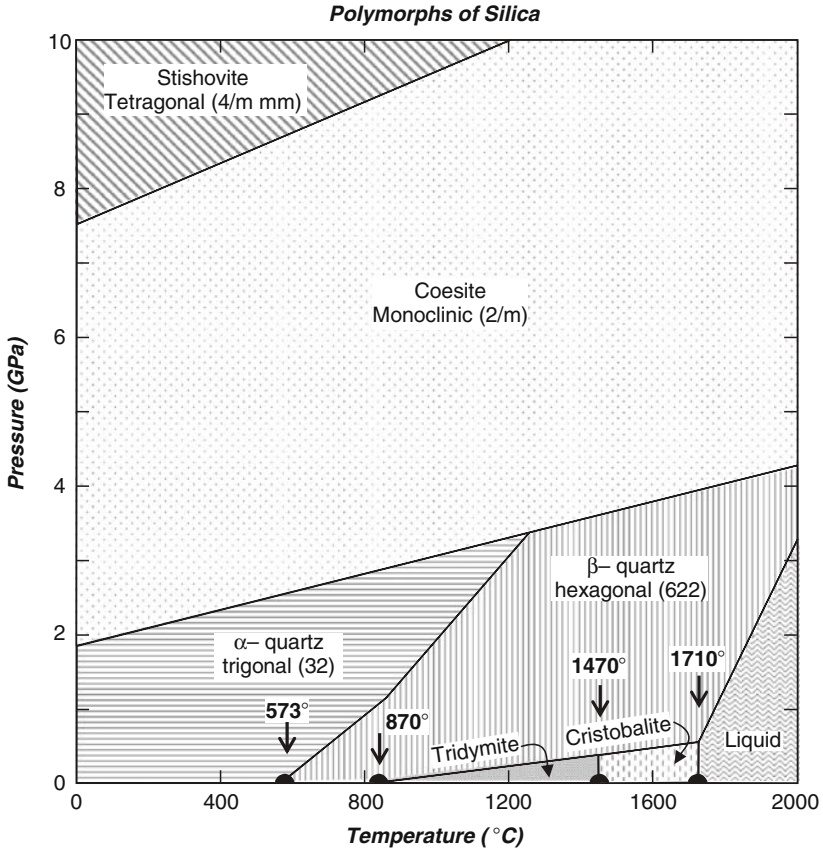

Fig. 2.1. Polymorphs of silica

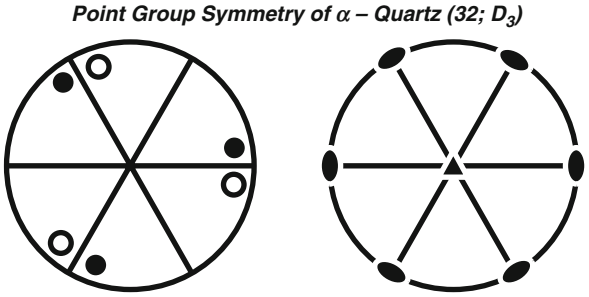

Fig. 2.2. Symmetry elements for α-quartz, point group 32

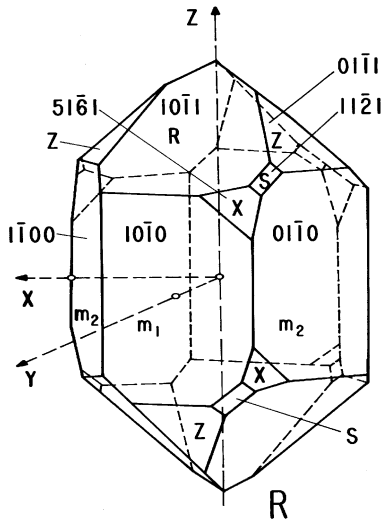

Fig. 2.3. Idealized, right-hand quartz, showing natural facets

move only 0.03 nm, changing the trigonal axis to hexagonal, and the point group symmetry to $622/D_6$. Beta quartz is also enantiomorphic, composed of space groups $P6_222/{D_6}^4$ and $P6_422/{D_6}^5$; handedness is preserved in the transition. Enantiomorphism implies the presence of piezoelectricity. Beta quartz is not stable below 573°C. At 600°C, unit cell dimensions are $a_0 = 0.501$ and $c_0 = 0.547$ nm, and density $\rho = 2.533$. α-tridymite (point group uncertain; mmm or 2/m) is metastable below 870°C, to ∼117°C; $\rho = 2.28$. β-tridymite (6/m mm) is stable between 870 and 1,470°C, and metastable down to ∼163°C; $\rho = 2.24$. α-cristobalite (422) is metastable to below 200°C; $\rho = 2.32$. β-cristobalite (m3m) is stable between 1,470 and 1,710°C, and metastable down to 268°C; $\rho = 2.24$. Density units are Mg/m^3. Coesite is of point symmetry 2/m; that of stishovite is 4/m mm; both are metastable under ordinary conditions. With the exception of α-cristobalite, the other phases are not piezoelectric. The symmetry diagram for β-quartz is given in Fig. 2.4.

Transitions between different phases of a single polymorph (α-β transformations) involve only bond warping, and not bond breaking; these displacive transformations proceed rapidly. Cooling through the α-β quartz transition invariably results in α-quartz regions having oppositely-directed x_1 axes: "electrical twinning." Transitions between polymorphs require breaking of bonds; these reconstructive transformations are slow, and subject to kinematic constraints.

Hydrothermal growth of cultured quartz takes place in aqueous NaOH or Na_2CO_3 solutions at temperatures of about 350°C and pressures between 80 and 200 MPa, driven by a temperature gradient from 4 to 10 K. The process

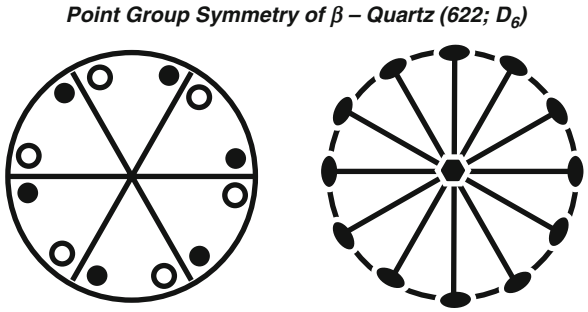

Fig. 2.4. Symmetry elements for β-quartz, point group 622

takes from one to nine months. Processing of quartz crystals includes the steps of cutting, X-ray orienting, lapping, polishing and etching (usually $NH_4F \cdot HF$ or $HF_{(aq)}$). Growth and etch rates are highly anisotropic, being most rapid along z, with the z rate between 100 and 1,000 times that along x or y axis.

2.2 Phenomenological Coefficients of Quartz

2.2.1 Matter Tensors and Symmetry

Voigt [25] considered field tensors, such as temperature, electric displacement, stress, and strain, and arranged the phenomenological coefficients (matter tensors) relating them according to their ranks. He made the simplification of converting the description of stress and strain from three-dimensional, second-rank tensors to six-dimensional vectors (first-rank tensors). This permits the description of linear elasticity, and related effects, such as piezoelectricity, in simple matrix form. Pertinent here are the intensive field tensors mechanical stress T, electric intensity E, the extensive field tensors mechanical strain S, and electric displacement D. Matter tensors appearing in the constitutive relations are, therefore, elastic stiffness c, and compliance s; dielectric permittivity ε, and impermeability β; and piezoelectric constants $d,\ e,\ g$, and h. A graphical portrayal of these relationships was first devised by Heckmann [26], and is now commonly used [1, 27, 28].

The extension of Hooke's Law to piezoelectric coupling between quasi-static mechanical and electrical variables is represented by 9×9 Van Dyke matrices. Four sets are commonly used, depending on the physical structure under consideration, as follows. A prime denotes matrix transpose.

Homogeneous sets:

(1) $S = s^{\mathrm{E}}\ T + d'\ E$ and $D = dT + \varepsilon^{\mathrm{T}} E$
(2) $T = c^{\mathrm{D}}\ S - h'\ D$ and $E = -hS + \beta^{\mathrm{S}} D$

Table 2.2. Van Dyke matrix for the mixed coefficients c^{E}, e, and ε^{S} of α-quartz

${c_{11}}^E$	${c_{12}}^E$	${c_{13}}^E$	${c_{14}}^E$	0	0	$-e_{11}$	0	0
${c_{12}}^E$	${c_{11}}^E$	${c_{13}}^E$	$-{c_{14}}^E$	0	0	e_{11}	0	0
${c_{13}}^E$	${c_{13}}^E$	${c_{33}}^E$	0	0	0	0	0	0
${c_{14}}^E$	$-{c_{14}}^E$	0	${c_{44}}^E$	0	0	$-e_{14}$	0	0
0	0	0	0	${c_{44}}^E$	${c_{14}}^E$	0	e_{14}	0
0	0	0	0	${c_{14}}^E$	${c_{66}}^E$	0	e_{11}	0
e_{11}	$-e_{11}$	0	e_{14}	0	0	${\varepsilon_{11}}^S$	0	0
0	0	0	0	$-e_{14}$	$-e_{11}$	0	${\varepsilon_{11}}^S$	0
0	0	0	0	0	0	0	0	${\varepsilon_{33}}^S$

Table 2.3. Van Dyke matrix for the homogeneous coefficients s^{E}, d, and ε^{T} of α-quartz

${s_{11}}^E$	${s_{12}}^E$	${s_{13}}^E$	${s_{14}}^E$	0	0	d_{11}	0	0
${s_{12}}^E$	${s_{11}}^E$	${s_{13}}^E$	$-{s_{14}}^E$	0	0	$-d_{11}$	0	0
${s_{13}}^E$	${s_{13}}^E$	${s_{33}}^E$	0	0	0	0	0	0
${s_{14}}^E$	$-{s_{14}}^E$	0	${s_{44}}^E$	0	0	d_{14}	0	0
0	0	0	0	${s_{44}}^E$	$2{s_{14}}^E$	0	$-d_{14}$	0
0	0	0	0	$2{s_{14}}^E$	${s_{66}}^E$	0	$-2d_{11}$	0
d_{11}	$-d_{11}$	0	d_{14}	0	0	${\varepsilon_{11}}^T$	0	0
0	0	0	0	$-d_{14}$	$-2d_{11}$	0	${\varepsilon_{11}}^T$	0
0	0	0	0	0	0	0	0	${\varepsilon_{33}}^T$

Mixed sets:

(3) $T = c^{\mathrm{E}}S - e'\ E$ and $D = eS + \varepsilon^{\mathrm{S}}E$
(4) $S = s^{\mathrm{D}}T + g'\ D$ and $E = -gT + \beta^{\mathrm{T}}D$

Constants d and g are "strain" coefficients; e and h are "stress" coefficients. The $[s^{\mathrm{E}},\ d',\ d,\ \varepsilon^{\mathrm{T}}]$ and $[c^{\mathrm{D}},\ -h',\ -h,\ \beta^{\mathrm{S}}]$ matrices are inverses, as are the $[c^{\mathrm{E}},\ -e',\ e,\ \varepsilon^{\mathrm{S}}]$ and $[s^{\mathrm{D}},\ g',\ -g,\ \beta^{\mathrm{T}}]$ matrices.

Point-group symmetry dictates the number of components appearing in the constitutive equations coupling the field tensors, and any relations among the components. Tables 2.2–2.5 display the Van Dyke matrices (or "term schemes") representing point group symmetry 32 and 622. Factors of 2 in the s, d, and g matrices arise from a convention regarding the definition of strain, and, in these tables, $\mathrm{c}_{12} = \mathrm{c}_{11} - 2\mathrm{c}_{66}$ and $\mathrm{s}_{12} = \mathrm{s}_{11} - \mathrm{s}_{66}/2$. The Van Dyke matrices of Tables 2.2 and 2.3, and of Tables 2.4 and 2.5 are inverses of each other.

2.2.2 Numerical Values for α-Quartz

2.2.2.1 Elastic Constants

Alpha-quartz possesses six independent elastic, two piezoelectric, and two dielectric constants. Two principal and competing conventions exist for

Table 2.4. Van Dyke matrix for the mixed coefficients c^{E}, e, and ε^{S} of β-quartz

${c_{11}}^E$	${c_{12}}^E$	${c_{13}}^E$	0	0	0	0	0	0
${c_{12}}^E$	${c_{11}}^E$	${c_{13}}^E$	0	0	0	0	0	0
${c_{13}}^E$	${c_{13}}^E$	${c_{33}}^E$	0	0	0	0	0	0
0	0	0	${c_{44}}^E$	0	0	$-e_{14}$	0	0
0	0	0	0	${c_{44}}^E$	0	0	e_{14}	0
0	0	0	0	0	${c_{66}}^E$	0	0	0
0	0	0	e_{14}	0	0	${\varepsilon_{11}}^S$	0	0
0	0	0	0	$-e_{14}$	0	0	${\varepsilon_{11}}^S$	0
0	0	0	0	0	0	0	0	${\varepsilon_{33}}^S$

Table 2.5. Van Dyke matrix for the homogeneous coefficients s^{E}, d, and ε^{T} of β-quartz

${s_{11}}^E$	${s_{12}}^E$	${s_{13}}^E$	0	0	0	0	0	0
${s_{12}}^E$	${s_{11}}^E$	${s_{13}}^E$	0	0	0	0	0	0
${s_{13}}^E$	${s_{13}}^E$	${s_{33}}^E$	0	0	0	0	0	0
0	0	0	${s_{44}}^E$	0	0	d_{14}	0	0
0	0	0	0	${s_{44}}^E$	0	0	$-d_{14}$	0
0	0	0	0	0	${s_{66}}^E$	0	0	0
0	0	0	d_{14}	0	0	${\varepsilon_{11}}^T$	0	0
0	0	0	0	$-d_{14}$	0	0	${\varepsilon_{11}}^T$	0
0	0	0	0	0	0	0	0	${\varepsilon_{33}}^T$

determining the signs of certain of the coefficients, and it is necessary to be consistent in following whichever choice is selected [16–22]. Table 2.6 contains experimental values for room-temperature elastic stiffnesses at constant electric field, c^{E} (isagric values). Recent results of James [32], indicate that measurement precision is now sufficient to distinguish among the small differences in values occurring between natural and cultured quartz, and between cultured varieties hydrothermally grown either with sodium hydroxide or with sodium carbonate mineralizer. Table 2.7 gives values for the isagric elastic compliances, s^{E} corresponding to the entries of Table 2.6.

2.2.2.2 Temperature Coefficients of Elastic Constants

It is found experimentally that a Taylor series expansion to the third order usually suffices to characterize the behavior of the elastic constants of quartz over the often-specified temperature range, −55°C to +90°C. The reference temperature, T_0, is usually taken to be room temperature. With y standing for any of the elastic stiffnesses or compliances, its value at temperature T is then given by

$$\Delta y/y_0 = T_y^{(1)}\ \Delta T + T_y^{(2)}\ (\Delta T)^2 + T_y^{(3)}\ (\Delta T)^3,$$

Table 2.6. Elastic stiffnesses, c^{E}

$c_{\lambda\mu}{}^{\mathrm{E}}$	[25]	[29][a]	[30]	[31]	[24][b]	[32]	[33][c]
c_{11}	85.48	86.75	86.74	86.80	86.80 ± 0.04	86.790	86.7997
c_{13}	14.36	11.3	11.91	11.91	11.91 ± 0.01	12.009	11.9376
c_{14}	−16.83	−17.96	−17.91	−18.04	-18.02 ± 0.07	−18.116	−18.0612
c_{33}	105.6	106.8	107.2	105.75	106.2 ± 0.8	105.79	105.7816
c_{44}	57.13	57.86	57.94	58.20	58.17 ± 0.13	58.212	58.2231
c_{66}	39.11	39.94	39.88	39.88	39.85 ± 0.03	40.000	39.8817
c_{12}	7.25	6.87	(6.98)	(7.04)	7.10 ± 0.09	6.7901	(7.0363)

unit: GPa
[a]Values of [34] corrected for piezoelectricity
[b]Averages gleaned from the literature
[c]Cultured quartz at 23°C

Table 2.7. Elastic compliances, s^{E}

$s_{\lambda\mu}{}^{\mathrm{E}}$	[25]	[29]	[30][a]	[31]	[24]	[32]	[33]
s_{11}	12.95	12.76	12.77	12.78	12.78	12.779	12.779
s_{13}	−1.53	−1.16	−1.22	−1.24	−1.23	−1.249	−1.238
s_{14}	4.31	4.52	4.50	4.52	−4.52	4.528	−4.525
s_{33}	9.88	9.61	9.60	9.74	9.69	9.736	9.733
s_{44}	20.04	20.09	20.04	19.98	19.99	19.997	19.983
s_{66}	29.28	29.10	29.12	29.17	29.18	29.102	29.172
s_{12}	−1.69	−1.79	−1.79	−1.81	−1.81	−1.772	−1.807

unit: $(\mathrm{TPa})^{-1}$
[a]Slightly different values are given in [36] and [37]

where $\Delta y = (y - y_0)$, $\Delta T = (T - T_0)$, and y_0 is the value of y at $T = T_0$. The coefficients $T_{\mathrm{y}}^{(\mathrm{n})}$ are the nth-order temperature coefficients (TCs) of y. Tables 2.8 and 2.9 contain values for the first-order TCs of the stiffnesses and compliances of quartz, respectively. In Tables 2.10 and 2.11 are given the second and third-order stiffness coefficients.

2.2.2.3 Piezoelectric Coefficients and Dielectric Permittivities

Table 2.12 contains values for the piezoelectric coefficients. Table 2.13 lists values for the dielectric permittivities and the impermeabilities, while Table 2.14 gives values for the thermoelastic (thermal expansion) coefficients.

2.2.2.4 Mass Density (ρ)

Natural quartz: $\rho = 2.6487$ at 20°C; 2.649 at 25°C [6]
Cultured quartz: $\rho = 2.6484 \pm 0.0002$ at 25°C [32]; unit: Mg m^{-3}

Table 2.8. First-order temperature coefficients of stiffnesses, $Tc_{\lambda\mu}{}^{(1)}$

$\lambda\mu$	[31]	[38]	[39]	[24][a]	[40]	[32]	[33][b]
11	−48.5	−44.3	−48.5	-46.4 ± 2.1	−68.2	−43.591	−45.5
13	−383	−492	−550	-476 ± 111	−705	−592.27	−745
14	105	98	101	105 ± 8	84.2	102.59	98.7
33	−153	−188	−160	-172 ± 24	−197	−190.32	−193
44	−158	−172	−177	-170 ± 13	−186	−171.59	−160
66	169	180	178	177 ± 8	158	176.79	166
12	−2,703	−2,930	−3,000[c]	$-2,901 \pm 183$		−2,640.1	(−2,443)

unit: 10^{-6}/K
[a] Averages gleaned from the literature
[b] Cultured quartz at 23°C
[c] −2,637 for consistency

Table 2.9. First-order temperature coefficients of compliances, $Ts_{\lambda\mu}{}^{(1)}$

λμ	[31]	[39]	[41]
11	16.5	15.5	8.5
13	−678	−166	−168.8
14	139.5	134	140
33	134.5	140	139.7
44	201	210	211.1
66	−138	−145	−151.9
12	−1,270	−1,370[a]	−1,296.5

unit: 10^{-6}/K
[a] −1,290 for consistency

Table 2.10. Second-order temperature coefficients of stiffnesses, $Tc_{\lambda\mu}{}^{(2)}$

λμ	[31]	[38]	[39]	[40]	[32]
11	−75	−407	−107	−117	−110.98
13	−2,000	−596	−1,150	−1,022	−1,218.5
14	−270	−13	−48	−54.4	−30.802
33	−187	−1,412	−275	−158	−165.31
44	−212	−225	−216	−272	−254.49
66	−5	201	118	152	156.18
12	−1,500	−7,245	−3,050[a]		−3,258.7

unit: 10^{-9}/K^2
[a] −2,678 for consistency

Table 2.11. Third-order temperature coefficients of stiffnesses, $Tc_{\lambda\mu}{}^{(3)}$

λμ	[31]	[38]	[39]	[40]	[32]
11	−15	−371	−70	−61.9	−99.879
13	600	−5,559	−750	−43.4	686.06
14	−630	−625	−590	−816	−459.28
33	−410	−243	−250	93.7	−19.089
44	−65	−190	−216	−45.6	−244.95
66	−167	−777	21	−239	102.80
12	1,910	4,195	−1,260[a]		−2,487.8

unit: $10^{-12}/\mathrm{K}^3$
[a] −1,110 for consistency

Table 2.12. Piezoelectric constants

	[38]	[30][a]	[33][b]	β-quartz [42]
d_{11}	2.37	2.31		
d_{14}	0.77	0.727		−1.86[c]
e_{11}	0.175	0.171	0.1719	
e_{14}	−0.0407	−0.0406	−0.0390	−0.067[c]
g_{11}		0.0578		
g_{14}		0.0182		
h_{11}		4.36		
h_{14}		−1.04		

units: d in pC/N; e in $\mathrm{C/m}^2$; g in m^2/C; h in N/nC
[30] derived from cgs, rounded
[a] Slightly different values are given in [36] and [37]
[b] Cultured quartz at 23°C; $\rho = 2.64867\,\mathrm{Mg/m}^3$
[c] At 612°C

Table 2.13. Dielectric permittivities, ε, and impermeabilities, β

	[30][a]	[32]	[33][a,b]
ε_{11}	39.21	39.16	39.136
ε_{33}	41.03	41.04	40.977
β_{11}	25.51	25.54	25.552
β_{33}	24.37	24.37	24.404

units: ε in pF/m; β in m/nF
[a] ε^{S}, β^{S}
[b] Cultured quartz at 23°C

Table 2.14. Thermoelastic constants, $\alpha^{(n)}$

	[39]	[43]	[32]	[44][a]	[33]
${\alpha_{11}}^{(1)}$	13.71	13.92	13.77	13.65	13.74
${\alpha_{33}}^{(1)}$	7.48	6.79	7.483	7.50	7.48
${\alpha_{11}}^{(2)}$	6.50	15.09	13.03	11.02	
${\alpha_{33}}^{(2)}$	2.90	8.69	9.405	8.00	
${\alpha_{11}}^{(3)}$	−1.90	−7.86	−6.329	−19.32	
${\alpha_{33}}^{(3)}$	−1.50	6.88	−5.440	−10.44	

units: $\alpha^{(1)}$ in 10^{-6}/K; $\alpha^{(2)}$ in 10^{-9}/K^2; $\alpha^{(3)}$ in 10^{-12}/K^3
[a] −50°C to +150°C

Table 2.15. Acoustic viscosities, η [46]

$\lambda\mu \rightarrow$	11	13	14	33	44	66	(12)
η	1.37	0.72	0.01	0.97	0.36	0.32	0.73

units: η in 10^{-3} Pa s (dekapoise)

- Thermoelastic constants, $\alpha^{(n)}$ See Table 2.14.
- Thermal diffusivity constants, $\alpha_{(td)}$; $\alpha_{(td)11} = 3.3$; $\alpha_{(td)33} = 6.1$; unit: $10^{-6}\,\mathrm{m}^2\,\mathrm{s}^{-1}$
- Specific heat capacity, c_p; $c_p = 740$; unit: J (kg-K)$^{-1}$
- Thermal conductivity, $k_{(th)}$; $k_{(th)} = \rho c_p \alpha_{(td)}$; $k_{(th)11} = 6.47$; $k_{(th)33} = 12.0$; unit: W (m-K)$^{-1}$
- Acoustic viscosity, η; unit: Pa s

Crystal quartz is often treated as lossless [16–21]; but at frequencies above 20 or 30 MHz, loss is usually dominated by internal friction. Lamb and Richter [46] determined acoustic viscosity η as the imaginary part of complex stiffness, $(c^{\mathrm{E}} + j\omega\eta)$. Values for the matrix elements of $\boldsymbol{\eta}$ are given in Table 2.15.

The quotient η/c is the motional time constant, τ_1, and its value is related to the limiting resonator Q due to intrinsic acoustic attenuation by the relation $Q = (\omega_0\tau_1)^{-1}$.

2.2.2.5 Third-Order Stiffnesses

Quartz resonator frequency shifts caused by environmental disturbances such as acceleration, static forces, and thermal transients have their genesis primarily in elastic nonlinearities. Plane-stress and thermal transient disturbances in quartz resonators may be reduced, or eliminated, by use of certain doubly rotated cuts, notably the BAW SC and SBTC cuts [2–4,51–54], and the SAW STC cut [55–57]. The necessary measurements of the 14 independent non-Hookean elastic stiffnesses of quartz were first made by Thurston, et al. [58]; see also [59, 60].

2.2.2.6 Recommended Values for α-Quartz

The comprehensive and readable works of Brice [24] and James [32] contain careful and insightful reviews of measurement methods, and of various data sets appearing in the literature. For the linear elastic, piezoelectric, and dielectric constants of quartz, the set obtained by Bechmann [30] using resonator methods is a good choice. The averaged values of Brice [24], and the set derived by James [32] from time-domain method measurements are good alternatives. For the temperature coefficients, the set given in [39], obtained from resonator measurements is a good choice, with the averaged values of Brice [24], and the set derived by James [32] from time-domain method measurements as good alternatives.

2.2.2.7 Beta-Quartz

Beta-quartz possesses five-independent elastic, one piezoelectric, and two dielectric constants, as well as ten independent third-order elastic constants. Table 2.16 lists the measured linear elastic stiffnesses and compliances of β-quartz. Table 2.12 contains the corresponding piezoelectric constants.

2.2.3 Piezoelectric Resonators

By far the greatest technological use of quartz is in piezoelectric resonators and transducers, including sensors. In the 1920s, and into the 1930s, extensional and flexural modes of thin bars and rods were used; in the 1930s into the 1940s, contour modes of plates and discs were used to achieve higher frequencies, since frequency is inversely proportional to the dimension determining the frequency. By the 1950s, driven by the need to reach still higher frequencies, thickness modes of thin plates were used almost exclusively [49, 110–114]. Obtaining requisite thinnesses by ordinary lapping and polishing techniques proved to be an obstacle to achieving fundamental frequencies in excess of about 50 MHz. Frequency requirements in the VHF and UHF ranges, and beyond, led to use of more modern microfabrication technologies that have enabled thickness modes to be realized in thin piezoelectric films.

Table 2.16. Elastic stiffnesses and compliances of β-quartz

$c^E_{\lambda\mu}$	[50]	$s^E_{\lambda\mu}$	[50]
c_{11}	116	s_{11}	9.41
c_{13}	33	s_{13}	−2.6
c_{33}	110	s_{33}	10.6
c_{44}	36	s_{44}	27.7
c_{66}	50	s_{66}	20.02
(c_{12})	16	s_{12}	−0.60

unit: c in GPa; s in $(\text{TPa})^{-1}$
$T = 600^\circ\text{C}$

2.2.4 Plate Resonator Cuts

To obtain desirable properties such as temperature compensation, high frequency resonator plates and films must have certain orientations with respect to the crystallographic axes of the crystal. A plate or film, with lateral dimensions large compared with the thickness, can be regarded as a plane, and specified by two orientation angles. Starting from a reference state where the plane normal is along the crystallographic y axis, one rotates the plane about the crystallographic z axis by an angle φ; the x axis of the plane, originally parallel to the crystallographic x axis, becomes the x' axis. Then, a second rotation is made about the new x' axis by angle θ, creating a compound, or doubly-rotated cut, or orientation. The notation for this operation is $(YXw\ell)\varphi/\theta$ [16]. When angle $\varphi = 0$, the cut is a rotated-Y-cut, with notation: $(YX\ell)\theta$. For further details, see [1, 4, 16, 48, 105, 106].

2.2.5 Equivalent Electrical Circuits

Piezoelectric resonators, filters, transducers, signal processors, sensors, and other acoustic components are invariably incorporated into using systems that are purely electrical. However, because the piezoelectric effect mediates between electrical and mechanical quantities, it is possible to describe the mechanical behavior of these components in purely electrical terms, and thereby to optimize the performance of the overall system. The simplest representation of a resonator is called the Butterworth-Van Dyke (BVD) circuit [107–109], which consists of a capacitor (C_0), representing the driving electrodes, shunted by a "motional" arm consisting of R_1 L_1 C_1 elements in series, representing acoustic loss, mechanical mass, and elastic spring, respectively, of the vibrating crystal. Circuit values depend on the material parameters, mode of motion, and geometry. For transducer applications, provision is made for the presence of mechanical ports in the appropriate equivalent circuits [35, 104–106].

A resonator, represented by the BVD circuit, appears as a capacitive reactance at frequencies below the region of resonance. As resonance is approached, the reactance first becomes zero ("resonance" frequency, f_R), passing into a region of inductive reactance, and reaching a very large value before returning to zero ("antiresonance" frequency, f_A), finally becoming capacitive again at higher frequencies. The region between f_A and f_R (the "pole – zero" spacing) is the normal operating region for an oscillator or filter. This spacing is proportional to the square of the piezoelectric coupling factor (k), discussed in the next paragraph. If this value is small, the oscillator frequency will be confined to a small range, and hence will be very stable; similarly, narrowband filters require small k values, and wideband filters require large k values.

2.2.6 Piezoelectric Coupling Factors

Piezoelectric coupling factors, k, are dimensionless measures of electromechanical energy transduction. In transducers and filters, they determine bandwidth

and insertion loss; in resonators and resonant MEMS devices, they establish pole-zero spacing and adjustment range; in actuators and sensors, they control electromechanical conversion efficiency. In applications, they usually appear as k^2. For a given type of resonant motion, effective values of elastic, piezoelectric, and dielectric coefficients arise. There are four basic forms expressing coupling, depending upon the constitutive equation set chosen. The generic homogeneous forms are the following:

- $k = |d|/\sqrt{(\varepsilon^{\mathrm{T}} s^{\mathrm{E}})}$ and $|h|/\sqrt{(\beta^{\mathrm{S}} c^{\mathrm{D}})}$. The generic mixed forms are:
- $k = |e|/\sqrt{(\varepsilon^{\mathrm{S}} c^{\mathrm{E}})}$ and $|g|/\sqrt{(\beta^{\mathrm{T}} s^{\mathrm{D}})}$ [28].

Explicit formulas for some α-quartz resonator plates are the following:

- X-cut (plate normal to x_1 axis): $k_{11} = |e_{11}|/\sqrt{[{\varepsilon_{11}}^{\mathrm{S}} {c_{11}}^{\mathrm{E}} + (e_{11})^2]} = 9.23\%$; pure extensional mode, driven by electric field in plate thickness direction.
- Y-cut (plate normal to x_2 axis): $k_{66} = |e_{11}|/\sqrt{[{\varepsilon_{11}}^{\mathrm{S}} {c_{66}}^{\mathrm{E}} + (e_{11})^2]} = 13.55\%$; pure shear mode, driven by electric field in plate thickness direction.
- Z-cut (plate normal to x_3 axis): $k_{44} = |e_{14}|/\sqrt{[{\varepsilon_{11}}^{\mathrm{S}} {c_{66}}^{\mathrm{E}}]} = 2.69\%$; pure shear mode, motion along direction of driving electric field in $x_2 - x_3$ plane.
- Rotated-Y-cuts (plate normal in $x_2 - x_3$ plane), pure shear mode: ${k_{26}}' = |{e_{26}}'|/\sqrt{[{\varepsilon_{22}}' c']}$; primes denote rotated values. AT cut: ${k_{26}}' = 8.80\%$ and BT cut: ${k_{26}}' = 5.62\%$. See Tables 2.17 and 2.18.

Table 2.17. Properties of AT and BT quartz cuts

Quantity	Unit	AT cut	BT cut
Angle	$(YX\ell)\theta$	$\theta = +35.25^\circ$	$\theta = -49.20^\circ$
Tf_{R}	$10^{-6}/\mathrm{K}$	0	0
$\partial Tf_{\mathrm{R}}/\partial\theta$	$10^{-6}/(K, \theta^\circ)$	−5.12	+2.14
$\lvert k\rvert$	%	8.80	5.62
v	km/s	3.322	5.073
Z	Mrayl	8.800	13.438
c'_{66}	GPa	29.24	68.16
e'_{26}	$\mathrm{C/m}^2$	−0.0949	−0.0931
ε'_{22}	pF/m	39.82	40.25

Table 2.18. Properties of other rotated-Y-cut quartz cuts

Quantity	Unit	Y cut	Max Tf_{R}	Min Tf_{R}	Z cut
Angle	$(YX\ell)\theta$	$\theta = 0^\circ$	$\theta = +4.03^\circ$	$\theta = +69.61^\circ$	$\theta = \pm 90^\circ$
Tf_{R}	$10^{-6}/\mathrm{K}$	+91.11	+94.00	−96.69	−78.53
$\partial Tf_{\mathrm{R}}/\partial\theta$	$10^{-6}/(\mathrm{K}, \theta^\circ)$	+0.583	0	0	+1.50
$\lvert k\rvert$	%	13.55	13.67	0.562	0
v	km/s	3.916	3.796	4.077	4.677

2.2.7 Properties of Selected α-Quartz Cuts

Table 2.17 contains data pertinent to the shear-mode AT and BT cuts, as these are the preponderant high frequency resonator orientations in current usage. Listed are Tf_{R}, resonance frequency TC; $\partial Tf_{\mathrm{R}}/\partial\theta$, angle gradient of Tf_{R}; $|k|$, effective coupling; v, acoustic velocity; $Z = \rho v$, acoustic impedance; and the related elastic ($c_{66}{}'$), piezoelectric ($e_{26}{}'$), and dielectric ($\varepsilon_{22}{}'$) values for these cuts. Table 2.18 lists $Tf_{\mathrm{R}}, |k|$, and v data for four other rotated-Y-cuts.

2.3 Innovations: Past and Future

2.3.1 History of Piezoelectric Materials [61]

The phenomenon of piezoelectricity has a very distinguished history. Coulomb conjectured its existence, and later both Haüy and Becquerel conducted unsuccessful experiments. The undoubted discoverers of the phenomenon were the Curie brothers. They knew what they were looking for, had the backgrounds and facilities to bring the search to a successful conclusion, and announced their 1880 discovery as follows [62]:

> "*Those crystals having one or more axes whose ends are unlike, that is to say hemihedral crystals with oblique faces, have the special physical property of giving rise to two electrical poles of opposite signs at the extremities of these axes when they are subjected to a change in temperature: this is the phenomenon known under the name of pyroelectricity.*
> "*We have found a new method for the development of polar electricity in these same crystals, consisting in subjecting them to variations in pressure along their hemihedral axes.*"

The name "piezoelectricity" was given by Hankel; Lippmann predicted the converse effect in 1881, and it was verified by the Curies the same year. Kelvin provided an atomic model in 1893 [63], and theories were advanced by Duhem and Pockels. In 1894, Voigt introduced the term "tensor" describing the phenomenological treatment of this and other effects in crystals. Langevin used Rochelle salt for sonar in the early 1910s, and Born theoretically calculated the piezoconstant of β-ZnS. Cady invented the quartz oscillator in the early 1920s. Tartrates and other water-soluble crystals with large piezoelectric values were investigated in the 1940s and 1950s [64], as were piezoceramics such as barium titanate and similar alloys [65]. Highly piezoelectric refractory oxides such as lithium niobate were introduced in the mid-1960s [66–68], followed by piezopolymers in the late 1960s [69], and isomorphs of quartz in the late 1990s [70–73]. Table 2.19 shows some of the major applications of piezoelectricity. Figure 2.5 portrays the nominal ranges of coupling and quality factor for the various classes of piezoelectrics mentioned. The range for piezopolymers is largely coextensive with that of piezo-semiconductors.

Table 2.19. Major applications of piezoelectricity

Communications and control	Industrial	Health and consumer	Newer applications
• Cellular radio • Television • Automotive radar	• Transducers • Sensors • Actuators • Pumps • Motors	• Transducers • Sensors • Actuators • Pumps • Motors	• Smart Structures • High Displacement Transducers • Mixed-effect Devices
– Signal processing – Frequency control and timing	– Ultrasonic cleaning – Sonar – Nondestructive evaluation (NDE)	– Noninvasive medical diagnostics – Hyperthermia – Lithotripsy	– Microelectromechanical (MEMS) devices – Microoptomechnaical (MOMS) devices
– Correlators			– Biomimetic devices
– Convolvers	– Liquid level sensors	– Subcutaneous medication	– Composite and functionally graded devices
– Filters	– Vibration damping	– Wristwatches	– Rainbow devices
– Delay lines	– High temperature sensors	– Camera focusing/steadying/ranging	– Acousto-photonic-electronic devices
– Oscillators	– Material properties determination	– Computer timing/printing/modems	
	– Chemical/biological sensors	– Ignition of gases (“spark pump”)	

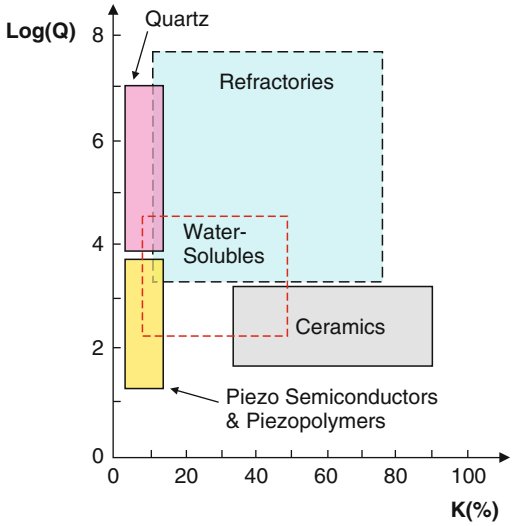

Fig. 2.5. Acoustic quality factor (Q) vs. piezoelectric coupling factor (k) for various types of piezoelectric materials

2.3.2 Current Quartz Uses

Acoustic materials are characterized primarily by elastic linearity, extremely low loss (high quality factor, Q), zero temperature coefficients (ZTCs) of frequency or delay, and particularly by the presence of piezoelectricity. Piezoelectricity provides a clean, efficient transduction mechanism mediating between mechanical motions and electric variables, using planar configurations available with conventional microelectronics fabrication technologies. Even compensation of stress and temperature-transient effects from elastic nonlinearities is possible with quartz, making available high stability bulk acoustic wave (BAW) oscillators. Surface acoustic wave (SAW) substrates provide conveniently accessible time axes for signal processing operations like convolution. The sonic/EM ratio (10^{-5}) affords severe miniaturization in both BAW and SAW devices. For many oscillator applications, it is necessary that the piezocoupling k not be large. This is because the oscillator operating point is confined to the resonator inductive region. Small coupling means a narrow inductive range, and concomitant high oscillator stability.

Acoustic device applications include wireless transceivers for voice, data, multimedia; spread-spectrum (SS) communications for wireless local area networks (WLANs) including WLAN robot, timing, and security applications; components in personal communications system (PCS) handsets, such as duplexers and voltage-controlled oscillators (VCOs); code division multiple access (CDMA) filters and timing; nonvolatile memories, and microelectromechanical (MEMS)/micro-optomechanical (MOMS) devices. Specific SAW applications are analog signal processing (convolvers, duplexers,

delay lines, and filters) for the mobile telecommunications, multimedia, and industrial-scientific-medical (ISM) bands; wireless passive identification tags, sensors and transponders, and microbalances. BAW applications include resonators in precision clock oscillators; front-end GPS filters for cell phones; thin-film, solidly mounted resonators (SMRs), and stacked crystal filters (SCFs) formed as SMRs, for integration with microwave heterojunction bipolar transistor (HBT) VCOs [5, 8–11].

2.3.3 Usage Considerations

Why quartz? Quartz is the only material known that possesses the following combination of desirable attributes:

- Piezoelectric
- Zero temperature coefficient cuts
- Stress/thermal transient compensated cuts
- Low acoustic loss/high acoustic Q
- Capable of withstanding 35,000–50,000 g shocks
- Very stable
- Capable of integration with micro- and nano-electronic components
- Easy to process; hard but not brittle; under normal conditions, low solubility in everything except fluoride etchants
- Abundant in nature; easy to grow in large quantities, at low cost, and with relatively high purity and perfection. Of the man-made single crystals, quartz, at over 3,000 tonnes per year (2000), is second only to silicon in quantity grown [7].

2.3.4 History of Innovations Related to Quartz that Led to Usages

- 1880
  - Piezoelectric effect discovered: Brothers Pierre & Jacques Curie
- 1900s
  - First hydrothermal growth of quartz in laboratory
- 1910s
  - First application of piezoelectricity, in sonar (Rochelle salt)
  - First quartz crystal oscillator, filter
- 1920s
  - Introduction of quartz resonator; requires “telescope making” technology: rough X-raying; grinding, lapping, polishing
  - Quartz resonator used for frequency stabilization and control
  - First crystal control of radio station
  - BVD equivalent circuit representation
  - Electrical measurements of resonators using oscillators
  - Compound resonator for measuring constants of nonpiezoelectrics
  - First quartz crystal-controlled clock

- 1930s
  - Temperature compensated bulk acoustic wave (BAW) AT/BT cuts developed; requires X-raying to minutes of arc
  - Modal surface motions investigated using lycopodium powder patterns
  - Equivalent circuit incorporating mechanical ports for transducers
- 1940s
  - Hydrothermal growth of quartz [74]; (Czochralski growth of Si and Ge)
  - Electrical measurements using passive transmission networks
  - Electrode system: Aℓ evaporation directly on resonator surfaces
  - Surface finish found to affect quality of resonator
  - First contoured, high-Q, resonator designs
  - Discussion of coupled plate modes [49]
- 1950s
  - Hydrothermal growth of cultured bars commercially viable
  - Solder-sealed metal enclosures
  - Processing ambient: soft vacuum
  - Quartz crystal microbalance (QCM) developed
  - Equivalent circuit in form of acoustic transmission line
  - Temperature-compensated crystal oscillator (TCXO) described
  - Theory of vibrations of anisotropic plates [110]
- 1960s
  - "Energy trapping" theory used to reduce unwanted modes [75–80]
  - Monolithic crystal filter (MCF) developed
  - Solidly mounted resonator (SMR) described
  - Glass enclosures introduced for low aging
  - Electrolytic sweeping reduces effects of ionizing radiation and neutron flux
  - Application of microelectronics technology enabling batch-processing
  - High coupling refractories, such as lithium niobate and tantalate grown
  - Anisotropic plate theory extended [111–113]
- 1970s
  - Cultured quartz use exceeded natural quartz; (Czochralski growth of III-V binaries)
  - Electrical measurements of crystal parameters using bridges
  - Stacked-crystal filters (SCFs) described
  - UV-ozone cleaning to produce atomically clean surfaces and very low aging [81]
  - Chemical polishing reduces subsurface damage; greatly increased shock resistance [82]
  - Temperature and nonlinear effects compensation; requires X-raying to seconds of arc
  - Interdigital transducer (IDT) enables efficient transduction of surface waves [83–87]
  - Surface acoustic wave (SAW) cuts; temperature compensated ST cut
  - Stress-compensated compound cut developed (SC) [2–4]

  - Electrical measurements using microcircuit bridges
  - Cold-weld metal enclosures
  - Processing ambient: cryo-pumps
  - Miniature tuning forks (∼32 kHz) enable quartz wristwatches
- 1980s
  - Stress-compensated BAW compound cut (SBTC) [52–54]
  - Stress-compensated SAW analog of SC cut (STC) [56]
  - Acceleration reduction in SAWs [57]
  - Ceramic flatpack enclosures; high temperature bakeout
  - Microprocessor-compensated crystal oscillator (MCXO) realized
  - Dual mode self-temperature sensing feature applied to MCXO
  - Coupled-mode cuts reduce temperature effects in wristwatch tuning forks
  - Electrode system: high precision air gaps
  - Electrical measurements using network analyzers
  - Processing ambient: ultra-high vacua
- 1990s and 2000s
  - Quartz analogues investigated
  - High stability environmental sensors developed; frequency counting inherently digital
  - Thin film resonator realized (TFR) [88–97]
  - Solidly mounted resonators (SMRs), advanced fabrication makes viable [89–91, 97]
  - Theory of compound-cut, contoured resonators [114]
  - Full-scale finite element method (FEM) models available for 3D simulation of modes

2.3.5 Future Innovations

2.3.5.1 Higher Frequencies

The push to higher frequencies is often dictated by bandwidth considerations. One important criterion by which to measure an acoustic material is its upper frequency limit; the concept is somewhat analogous to the cutoff frequency used for assessing transistors. Maximum usable frequency ($f_{\max}$) for a piezoelectric resonator is determined jointly by the piezocoupling factor (k) and the acoustic time constant, τ_1. The relation is $f_{\max} = 2k^2/(\pi^3\tau_1)$, where $\tau_1 = (2\pi f_o Q)^{-1}$, and Q is the measured acoustic quality factor at f_o, the nominal operating frequency [98]. A figure of merit (FOM) often used for piezofilters is (Qk^2) [95]. Thus $f_{\max} = [(4f_0/\pi^2) \cdot (\text{FOM})]$. Put another way, the resonant structure approaches the limit of its usefulness at a normalized frequency ($f_{\max}/f_0$) approximately 40% of the FOM. A quartz CDMA filter at the 1.9 GHz PCS band typically has an FOM of 120, indicating that

such devices are intrinsically capable of operation at much higher frequencies. Values of $f_{\max}$ from measurements of attenuation and piezocoupling are much higher than frequencies encountered in practice. The discrepancy relates primarily to manufacturing technology, rather than inherent material limitations. For example, AT-cut quartz with $\tau_1 = 11.8\,\text{fs}$ and $k = 8.80\%$, yields $f_{\max} = 42.3\,\text{GHz}$, a value exceeding present capabilities, but an achievable goal for the future [99].

2.3.5.2 High Coupling Isomorphs of Quartz [70–73]

The search for new materials is fed by practical demands for devices with improved characteristics, e.g., lower loss (higher resonator quality factor (Q), lower filter insertion loss (IL)), higher piezocoupling (k^2) for increased filter bandwidth, better temperature stability, greater miniaturization (higher acoustic velocity), etc. Materials receiving recent attention include the quartz analog langasite and its isomorphs, generically called LGX.

The langasite (LGS, $La_3Ga_5SiO_{14}$) family consists of Czochralski grown, congruently melting, class 32 materials such as langanite (LGN, $La_3Ga_{11/2}Nb_{1/2}O_{14}$) and langatate (LGT, $La_3Ga_{11/2}Ta_{1/2}O_{14}$) [70,71]. Table 2.20 provides pertinent phenomenological data. These materials have acoustic Qs higher than quartz, but have disordered structures, due to the difficulty of satisfying both ionic size and charge compensation constraints. In the future, totally ordered $(Ca, Sr)_3(Nb, Ta)Ga_3Si_2O_{14}$ crystals, and similar members, are expected to offer higher elastic stiffnesses, as well as lower dielectric permittivity and higher piezocoupling. Candidate materials include CNGS ($Ca_3NbGa_3Si_2O_{14}$), CTGS ($Ca_3TaGa_3Si_2O_{14}$), SNGS ($Sr_3NbGa_3Si_2O_{14}$), and STGS ($Sr_3TaGa_3Si_2O_{14}$). Main market possibilities are greater bandwidth (versus quartz), high stability IF filters; high temperature sensors (no twinning); and high Q BAW and SAW resonators [72].

2.3.5.3 Epitaxial Growth of Quartz and Isomorphs

Future miniaturization goals demanded for micro and nano-electromechanical systems (MEMS, NEMS) development [100,101] will require newer methods of growth and fabrication of thin quartz films and membranes. Recent advances in low-pressure vapor-phase epitaxy [102, 103] open exciting new avenues for future development. Extension of this and other new growth methods applied to quartz and its analogues, such as the totally-ordered LGX family, may yield largely defect-free crystal lattices, and the possibility of achieving greater isotopic constituent purity. Both advances would reduce phonon scattering, realizing significantly higher acoustic Qs, and thereby also further raise the achievable maximum useable frequency [45, 47].

Table 2.20. Material constants of langasite and isomorphs

Quantity	Langasite (LGS)	Langanite (LGN)	Langatate (LGT)
Elastic stiffnesses, $c_{\lambda\mu}{}^{\mathrm{E}}$ (GPa)			
c_{11}	188.49	192.99	188.52
c_{13}	96.88	102.25	103.36
c_{14}	14.15	14.85	13.51
c_{33}	261.68	264.65	261.80
c_{44}	53.71	49.56	51.10
c_{66}	42.21	41.16	40.32
Temperature coefficients of stiffnesses, $Tc_{\lambda\mu}{}^{\mathrm{E}}$ (10^{-6}/K)			
Tc_{11}	−43.91	−56.34	−78.24
Tc_{13}	−61.95	−31.27	−111.40
Tc_{14}	−309.10	−478.90	−359.60
Tc_{33}	−91.90	−114.70	−102.30
Tc_{44}	−44.05	−14.14	+21.65
Tc_{66}	−22.43	+15.25	−43.63
Piezoelectric stress constants, $e_{\mathrm{m}\lambda}$ (C/m^2)			
e_{11}	−0.402	−0.452	−0.456
e_{14}	+0.130	+0.061	+0.094
Dielectric permittivities, $\varepsilon_{\mathrm{ij}}/\varepsilon_0$ (dimensionless)			
$\varepsilon_{11}/\varepsilon_0$	19.62	20.09	18.27
$\varepsilon_{33}/\varepsilon_0$	49.41	79.34	78.95
Mass density, ρ (Mg/m^3)			
ρ	5.739	6.029	6.150
Thermoelastic coefficients, α_{ij} (10^{-6}/K)			
α_{11}	5.63	6.67	6.09
α_{33}	4.08	5.06	3.83

References

1. W.G. Cady, *Piezoelectricity* (McGraw-Hill, New York, 1946)
2. E.P. EerNisse, in *Proc. 29th Ann. Freq. Control Symp.*, pp. 1–4, US Army Electronics Command, Ft. Monmouth, NJ, May 1975
3. J.A. Kusters, J. Leach, in *Proc. IEEE.* vol. 65, no. 2, pp. 282–284, February (1977)
4. A. Ballato, in *Physical Acoustics: Principles and Methods*, vol. 13, ed. by W.P. Mason, R.N. Thurston. (Academic Press, New York, 1977), Chap. 5, pp. 115–181, ISBN: 0-12-477913-1
5. S. R. Stein, J. R. Vig, in *The Froelich/Kent Encyclopedia of Telecommunications*, Vol. 3, ed. by F.E. Froehlich, A. Kent (Marcel Dekker, New York, 1992) pp. 445–500
6. R.B. Sosman, *The Properties of Silica* (Chemical Catalog Co., New York, 1927)
7. "Quartz crystal," Bulletin 667, Mineral Facts and Problems, US Department of the Interior, Bureau of Mines, 1975

8. A. Ballato, J. R. Vig, in *Encyclopedia of Applied Physics*, Vol. 14, ed. by G. Trigg (VCH Publishers, New York, 1996), pp. 129–145, ISBN: 3-527-28136-3
9. D.J. Jones, S.E. Prasad, J.B. Wallace, Key Eng. Mater. **122–124**, 71–144, (1996)
10. IEEE Trans. Microwave Theory Tech. **49**(4), part II, 741–847 (April 2001). Special Issue on Microwave Acoustic Wave Devices for Wireless Communications and Sensing. R. Weigel and K. Hashimoto, guest editors
11. R. Weigel, D.P. Morgan, J.M. Owens, A. Ballato, K.M. Lakin, K. Hashimoto, C. C. W. Ruppel, IEEE Trans. Microwave Theory Tech. **50**(3), 738–749 (March 2002)
12. C. Frondel, *Dana's System of Mineralogy, Volume II: Silica Minerals*, (Wiley, New York, 1962)
13. B.K. Vainshtein, *Fundamentals of Crystals: Symmetry, and Methods of Structural Crystallography*, 2nd edn. (Springer-Verlag, Berlin, 1994), ISBN 3-540-56558-2
14. B.K. Vainshtein, V.M. Fridkin, V.L. Indenbom, *Modern Crystallography II*, (Springer-Verlag, Berlin, 1982), ISBN 3–540–10517–4
15. C. Klein, C.S. Hurlbut, Jr., *Manual of Crystallography (after J.D. Dana)*, 21st edn. revised, (Wiley, New York, 1999), ISBN: 0-471-31266-5
16. "IRE Standards on piezoelectric crystals, 1949," Proc. IRE, vol. 37, no. 12, pp. 1378–1395, December 1949. (IEEE Standard no. 176)
17. "IRE standards on piezoelectric crystals: determination of the elastic, piezoelectric, and dielectric constants - the electromechanical coupling factor, 1958," Proc. IRE, vol. 46, no. 4, pp. 764–778, April 1958. (IEEE Standard no. 178)
18. "IRE standards on piezoelectric crystals – the piezoelectric vibrator: definitions and methods of measurements, 1957," Proc. IRE, vol. 45, no. 3, pp. 353–358, March 1957
19. "Standard definitions and methods of measurement for piezoelectric vibrators," IEEE Standard no. 177, (IEEE, New York, May 1966)
20. "IEEE Standard on piezoelectricity," IEEE Standard 176–1978, IEEE, New York. Reprinted in IEEE Trans. Sonics Ultrason., vol. SU-31, no. 2, Part 2, 55 pp., March 1984
21. "IEEE Standard on piezoelectricity," IEEE Standard 176–1987, IEEE, New York
22. T.R. Meeker, in *Proc. 33rd Annual Frequency Control Symp.*, pp. 176–180, (Atlantic City, NJ, May-June 1979)
23. L. Pauling, *The Nature of the Chemical Bond*, 3rd edn. (Cornell University Press, Ithaca, 1960). ISBN: 0-8014-0333-2
24. J.C. Brice, Revs. Mod. Phys. **57**(1), 105–146 (January 1985)
25. W. Voigt, *Lehrbuch der Kristallphysik* (B.G. Teubner, Leipzig, 1928)
26. G. Heckmann, Ergeb. exakt. Naturwiss. **4**, 100–153 (1925)
27. J.F. Nye, *Physical Properties of Crystals* (Oxford University Press, Oxford, 1985). ISBN: 0-19-851165-5
28. A. Ballato, IEEE Trans. Ultrason., Ferroelec., Freq. Contr., **42**(5), 916–926 (September 1995)
29. A.W. Lawson, Phys. Rev. **59**, 838–839 (1941)
30. R. Bechmann, Phys. Rev. **110**(5), 1060–1061 (June 1, 1958)
31. W.P. Mason, Bell Syst. Tech. J. **30**, 366–380 (April 1951)

32. B.J. James, "Determination of the Elastic and Dielectric Properties of Quartz," PhD Dissertation, Royal Holloway and Bedford New College, University of London, Spring 1987, 231 pp. See also B. J. James, "A new measurement of the basic elastic and dielectric constants of quartz," IEEE Intl. Frequency Control Symp. Proc. (42nd Ann.), pp. 146–154, Baltimore, MD, June 1988
33. J. Kushibiki, I. Takanaga, S. Nishiyama, IEEE Trans. Ultrason., Ferroelect., Freq. Contr. **49**(1), 125–135 (January 2002)
34. J.V. Atanasoff, P. J. Hart, Phys. Rev. **59**(1), 85–96 (1941)
35. W.P. Mason, Phys. Rev. **55**, 775–789 (April 1939)
36. R. Bechmann, Proc. Phys. Soc. (London), **B64**, 323–337 (April 1951)
37. R. Bechmann, Archiv der Elektrischen Übertragung **5**, 89–90 (1951). (present name: Archiv für Elektronik und Übertragungstechnik)
38. I. Koga, M. Aruga, Y. Yoshinaka, Phys. Rev. **109**, 1467–1473 (March 1958)
39. R. Bechmann, A. Ballato, T. J. Lukaszek, Proc. IRE **50**(8), 1812–1822 (August 1962); Proc. IRE **50**(12), 2451 (December 1962)
40. P.C.Y. Lee, Y.-K. Yong, J. Appl. Phys. **60**(7), 2327–2342 (1986)
41. J. Zelenka, P.C.Y. Lee, IEEE Trans. Sonics Ultrason. SU-**18**(2), 79–80 (1971)
42. R.K. Cook, P.G. Weissler, Phys. Rev. **80**(4), 712–716 (15 November 1950)
43. A. Ballato, M. Mizan, IEEE Trans. Sonics Ultrason. SU-**31**(1), 11–17 (January 1984)
44. J.A. Kosinski, J.G. Gualtieri, A. Ballato, IEEE Trans. Ultrason., Ferroelec., Freq. Control **39**(4), 502–507 (July 1992)
45. R. Bechmann, in *Landolt-Börnstein, Numerical Data and Functional Relationships in Science and Technology, New Series, Group III: Crystal and Solid State Physics*, ed. by K.–H. Hellwege, A.M. Hellwege (Springer Verlag, Berlin, New York, vol. III/1, pp. 40–123, 1966; and vol. III/2, pp. 40–101, 1969)
46. J. Lamb, J. Richter, Proc. Roy. Soc. (London) **A293**, 479–492 (1966)
47. W.R. Cook, Jr., H. Jaffe, in *Landolt-Börnstein, Numerical Data and Functional Relationships in Science and Technology, New Series, Group III: Crystal and Solid State Physics*, vol. III/11, ed. by K.–H. Hellwege, A.M. Hellwege (Springer Verlag, Berlin, New York, 1979) pp. 287–470
48. B. Parzen, *Design of Crystal and Other Harmonic Oscillators* (Wiley, New York, 1983). ISBN: 0-471-08819-6
49. R.A. Sykes, in *Quartz Crystals for Electrical Circuits: Their Design and Manufacture*, ed. by R.A. Heising (D. Van Nostrand, New York, 1946) Chap. 6, pp. 205–248
50. E.W. Kammer, T.E. Pardue, H.F. Frissel, J. Appl. Phys. **19**(3), 265–270 (March 1948)
51. B.K. Sinha, Ferroelectrics **41**(1), 61–73 (1982)
52. B.K. Sinha, Proc. 35th Annu. Freq. Control Symp. 213–221 (May 1981)
53. M. Valdois, B.K. Sinha, J.-J. Boy, IEEE Trans. Ultrason., Ferroelec., Frequency Contr. **36**(6), 643–651 (November 1989)
54. B.K. Sinha, IEEE Ultrason. Symp. Proc. 557–563 (December 1990)
55. B.K. Sinha, IEEE Trans. Sonics Ultrason. SU-**32**(4), 583–591 (July 1985)
56. B.K. Sinha, IEEE Trans. Ultrason., Ferroelec., Frequency Contr. **34**(1), 64–74 (January 1987)
57. S. Locke, B. K. Sinha, IEEE Trans. Ultrason., Ferroelec., Frequency Contr. UFFC-**34**(4), 478–484 (July 1987)
58. R.N. Thurston, H.J. McSkimin, P. Andreatch, Jr., J. Appl. Phys. **37**(1), 267–275 (January 1966)

59. R. Stern, R.T. Smith, J. Acoust. Soc. Am. **44**, 640–641 (1968)
60. R.F.S. Hearmon, in Landolt-Börnstein, Numerical Data and Functional Relationships in Science and Technology, New Series, Group III: Crystal and Solid State Physics, vol. III/11, ed. by K.–H. Hellwege, A.M. Hellwege (Springer Verlag, Berlin, New York, 1979) pp. 245–286
61. W.P. Mason, J. Acoust. Soc. Am. **70**(6), 1561–1566 (December 1981)
62. P. Curie et, J. Curie, Bull. Soc. Fr. Mineral. Cristallogr. **3**, 90–93 (1880); C. R. Acad. Sci. (Paris) **91**, 294, 383 (March 1880)
63. M. Trainer, Eur. J. Phys. **24**(5), 535–542 (September 2005)
64. R. Bechmann, et al., in *Piezoelectricity* (Her Majesty's Stationery Office, London, 1957), 369 pp
65. D. Berlincourt, J. Acoust. Soc. Am. **70**(6), 1586–1595 (December 1981)
66. T. Yamada, N. Niizeki, H. Toyoda, Japan. J. Appl. Phys. **6**(2), 151–155 (1967)
67. A.W. Warner, M. Onoe, G.A. Coquin, J. Acoust. Soc. Am. **42**(6), 1223–1231 (December 1967)
68. R.T. Smith, F. S. Welsh, J. Appl. Phys. **42**(6), 2219–2230 (May 1971)
69. G.M. Sessler, J. Acoust. Soc. Am. **70**(6), 1596–1608 (December 1981)
70. R.C. Smythe, IEEE Intl. Frequency Control Symp. Proc. 761–765 (May 1998)
71. D.C. Malocha, M.P. da Cunha, E. Adler, R.C. Smythe, S. Frederick, M. Chou, R. Helmbold, Y.S. Zhou, 2000 IEEE/EIA Intl. Freq. Control Symp. Proc., pp. 201–205, Kansas City, MO, June 2000
72. B.H.T. Chai, A.N.P. Bustamante, M. C. Chou, "A new class of ordered langasite structure compounds," 2000 IEEE/EIA Intl. Freq. Control Symp. Proc., pp. 163–168, Kansas City, MO, June 2000
73. P.W. Krempl, J. Phys. IV France **126**, 95–100 (June 2005)
74. F. Iwasaki, H. Iwasaki, J. Crystal Growth, **237–239**, 820–827 (2002)
75. W. Shockley, D.R. Curran, D.J. Koneval, Proc. 17th Ann. Frequency Control Symp. 88–126 (May 1963)
76. D.R. Curran, D.J. Koneval, Proc. 18th Ann. Freq. Control Symp. 93–119 (May 1964)
77. W.S. Mortley, Wireless World **57**, 399–403 (October 1951)
78. W.S. Mortley, Proc. IEE (London) **104B**, 239–249 (December 1956)
79. R.D. Mindlin, J. Acoust. Soc. Am. **43**(6), 1329–1331 (June 1968)
80. H.F. Tiersten, R.C. Smythe, J. Acoust. Soc. Am. **65**(6), 1455–1460 (June 1979)
81. J.R. Vig, J.W. Le Bus, IEEE Trans. Parts, Hybrids, Packaging **PHP-12**(4), 365–370 (December 1976)
82. J.R. Vig, J.W. LeBus, R.L. Filler, Proc. 31st Ann. Freq. Control Symp. 131–143 (June 1977)
83. R.M. White, F.W. Voltmer, Appl. Phys. Lett. **7**(12), 314–316 (1965)
84. M.B. Schulz, B.J. Matsinger, M.G. Holland, J. Appl. Phys. **41**(7), 2755–2765 (1970)
85. R.M. White, Proc. IEEE **58**(8), 1238–1276 (August 1970)
86. M.G. Holland, L.T. Claiborne, Proc. IEEE **62**(5), 582–611 (May 1974)
87. B.K. Sinha, H.F. Tiersten, Appl. Phys. Lett. **34**(12), 817–819 (15 June 1979)
88. N.F. Foster, J. Acoust. Soc. Am. **70**(6), 1609–1614 (December 1981)
89. W.E. Newell, Proc. IEEE **52**(12), 1603–1607 (December 1964)
90. W.E. Newell, Proc. IEEE **53**(6), 575–581 (June 1965)
91. W.E. Newell, Proc. IEEE **53**(10), 1305–1308 (October 1965)
92. A. Ballato, T. Lukaszek, Proc. IEEE **51**(10), 1495–1496 (October 1973)

93. A. Ballato, H.L. Bertoni, T. Tamir, IEEE Trans. Microwave Theory Tech. **MTT-22**(1), 14–25 (January 1974)
94. K.M. Lakin, G.R. Kline, R.S. Ketcham, J.T. Martin, K.T. McCarron, IEEE Intl. Freq. Control Symp. Proc. 536–543 (May-June 1989)
95. K.M. Lakin, IEEE Intl. Freq. Control Symp. Proc. 201–206 (May 1991)
96. K.M. Lakin, G.R. Kline, K.T. McCarron, IEEE MTT-S Intl. Microwave Symp. Digest **3**, 1517–1520 (June 1993)
97. K.M. Lakin, IEEE Microwave Magazine **4**(4), 61–67 (December 2003)
98. A. Ballato, J.G. Gualtieri, IEEE Trans. Ultrason., Ferroelect., Freq. Cont. **41**(6), 834–844 (November 1994)
99. H. Iwata, IEICE Electronics Express **1**(12), 346–351 (September 2004)
100. K.L. Ekinci, M.L. Roukes, Rev. Sci. Instrum. **76** art. 061101, 12pp. (2005)
101. MEMS: A Practical Guide to Design, Analysis, and Applications, ed. by J.G. Korvink, O. Paul (Springer-Verlag, Heidelberg 2006), ISBN: 3-540-21117-9
102. N. Takahashi, T. Nakumura, S. Nonaka, H. Yagi, Y. Sinriki, K. Tamanuki, Electrochemical and Solid State Lett. **6**(5), C77–C78 (2003)
103. N. Takahashi, T. Nakumura, Electrochemical and Solid State Lett. **6**(11), H25–H26 (2003)
104. A. Ballato, IEEE Trans. Ultrason., Ferroelect., Freq. Contr., **48**(5), 1189–1240 (September 2001)
105. R. A. Heising (ed.), *Quartz Crystals for Electrical Circuits: Their Design and Manufacture* (D. Van Nostrand, New York, 1946)
106. W.P. Mason, *Piezoelectric Crystals and their Application to Ultrasonics* (Van Nostrand, New York, 1950)
107. A. Ballato, Proc. IEEE **58**(1), 149–151 (January 1970)
108. B.A. Auld, *Acoustic Fields and Waves in Solids*, Vol. I and II, (Robert E. Krieger Publishing, Malabar, FL, 1990). ISBNs: 0-89874-783-X; 0-89874-782-1
109. W.P. Mason, Proc. IEEE **57**(10), 1723–1734 (October 1969)
110. R.D. Mindlin, J. Appl. Phys., **23**(1), 83–88 (January 1952)
111. R.D. Mindlin, D.C. Gazis, Proc. Fourth U. S. Natl. Congr. Appl. Math. 305–310 (1962)
112. R.D. Mindlin, P.C.Y. Lee, Intl. J. Solids and Struct. **2**(1), 125–139 (January 1966)
113. R.D. Mindlin, W.J. Spencer, J. Acoust. Soc. Am. **42**(6), 1268–1277 (December 1967)
114. B.K. Sinha, IEEE Trans. Ultrason., Ferroelec., Frequency Contr. **48**(5), 1162–1180 (September 2001)

http://www.springer.com/978-3-540-68680-4

Piezoelectricity
Evolution and Future of a Technology
Heywang, W.; Lubitz, K.; Wersing, W. (Eds.)
2008, XVIII, 582 p., Hardcover
ISBN: 978-3-540-68680-4